Check for updates

High sulfur content composite materials from renewable fatty acid cellulose esters (FACEs) *via* inverse vulcanization†

Timo Sehn,[a] Julian Fanelli, [ID] [a] Lisa Wahl[a] and Michael A. R. Meier [ID] *[ab]

Herein, we introduce an efficient inverse vulcanization of fully renewable cellulose-based monomers. Therefore, biobased fatty acid cellulose esters (FACEs) with different degrees of substitution ($0.38 \leq DS \leq 0.62$) were inversely vulcanized to obtain high sulfur content composite materials (~95 wt% sulfur). In-depth structural characterization of the crosslinked sections *via* differential scanning calorimetry (DSC), thermogravimetric analysis (TGA), energy dispersive X-ray (EDX) spectroscopy, and scanning electron microscopy (SEM) revealed an increased amount of covalently incorporated sulfur (5.67 wt% $\leq$ sulfur wt% ≤ 56.2 wt%) with a higher DS of FACEs. Investigating structure–property relationships further revealed an increase in thermal stability ($227\ °C \leq T_{d,5\%} \leq 247\ °C$) accompanied by a decreased wettability ($87° \leq \theta \leq 99°$) with DS. The obtained materials showed application possibilities for water purification, *i.e.* for mercury extraction ($70\% \leq Hg_{removal}^{2+} \leq 95\%$).

Sustainability spotlight

Sulfur is an abundant waste material, it is directly used as the main component (95% content) in inverse vulcanized materials based on a fully renewable polymer network derived from fatty acids and cellulose. Material properties and especially the network structure of the composite materials were characterized in detail. The obtained materials showed promising application possibilities in the field of water purification, related to the important sustainable development goal of clean water. The described materials were able to efficiently remove mercury ions.

Introduction

The development of more sustainable synthetic approaches, targeting polymeric materials with tailor made properties, remains of high importance. The 12 principles of green chemistry, established by Anastas and Warner in 1998,[1,2] have to serve as guidelines and should not be contradicted to achieve this goal. Key aspects of these principles include the utilization of renewable feedstocks and catalysts accompanied by an improved energy efficiency along with the avoidance of waste and toxic chemicals.[1,2]

The ongoing extensive depletion of petroleum resources underscores the importance of renewable feedstocks in material synthesis. Thus, cellulose, as the most abundant biopolymer on earth (1.5×10^{12} tons p.a.), is a relevant renewable platform chemical, as it offers unique properties such as

biodegradability, biocompatibility and high mechanical and thermal stability.[3–5] However, cellulose modification remains challenging due to the limited processability and solubility in common organic solvents.[6–8] At a molecular level, extensive intra- and intermolecular hydrogen bonding interactions between the hydroxyl groups of the cellulose backbone (consisting of β-1,4 linked glucose units) induce the limited processability and solubility.[9]

Several heterogeneous and homogeneous modification approaches for cellulose derivatization are established.[3,10,11] On one hand, cellulose modification in a heterogeneous fashion is mainly employed in industry and suffers from drawbacks such as backbone degradation induced by harsh reaction conditions or uneven distribution of the introduced side chains along the polymer backbone.[3,11] In contrast, homogeneous modification approaches for cellulose using polar solvent systems such as LiCl/DMAc,[12,13] ionic liquids (ILs, *e.g.* 1-butyl-3-methyl-imidazoliumchloride[14] or 1-ethyl-3-methyl-imidazolium 2-pyridinolate),[9] or so-called switchable solvent systems overcome the above mentioned challenges, *i.e.* backbone degradation and uneven distribution of the side chains, and furthermore allow for a straightforward adjustment of the degree of substitution (DS).[3,5] The DS is defined as the amount of substituted hydroxyl

[a]*Institute of Biological and Chemical Systems – Functional Molecular Systems (IBCS-FMS), Karlsruhe Institute of Technology (KIT), Karlsruhe 76131, Germany. E-mail: m.a.r.meier@kit.edu*

[b]*Institute of Organic Chemistry (IOC), Karlsruhe Institute of Technology (KIT), Kaiserstraße 12, Karlsruhe 76131, Germany*

groups per anhydroglucose unit (AGU) and can vary between 0 and 3 for native and fully modified cellulose, respectively.

Cellulose esters (CE) have emerged as the most important cellulose derivatives, since this material class is already employed as a biobased alternative to fossil-based polymers in membranes, food packages and coatings.[3,15,16] Especially in terms of sustainability, fully renewable materials such as fatty acid cellulose esters (FACEs), where cellulose is modified with a second biobased substrate derived from a vegetable oil, have received significant attention within the last few years.[7,15] However, to truly classify materials such as FACEs as more sustainable than others, the complete synthetic approach must be considered.

To better quantify the environmental impact of chemical processes, the E-factor (taking reagents, yield, side products and solvent losses into account), which is defined as the mass ratio of the desired product and the produced waste, was introduced.[17] Nevertheless, the E-factor does not provide any information about toxicity, which is a key aspect of the 12 principles of green chemistry and is crucial in terms of adhering to safety regulations.[1,2]

Accordingly, when assessing how sustainable certain FACEs are, especially the recyclability of the solvent system and the fatty acid derivative used in the approach must be considered. In most of the synthetic procedures for the synthesis of FACEs, activated fatty acid derivatives, i.e. fatty acid chlorides,[18,19] N,N'-carbonyldiimidazole (CDI) activated fatty acids[20,21] or fatty acid anhydrides,[22] are employed. These activated fatty acid derivatives suffer from drawbacks including highly unsustainable synthesis procedures, i.e. including phosgene derived activating agents such as CDI, or the release of toxic or corrosive byproducts during the modification processes, i.e. hydrochloric acid (HCl).[15,23] More sustainable reagents for the synthesis of FACEs are vinyl and methyl fatty acid esters, as their production can be achieved in a considerably more sustainable manner and the released compounds can be captured during the modification processes.[24,25] Regarding the recyclability of the employed solvent system, especially ILs possess limitations, due to their easy contamination.[3,26] However, according to the literature, the derivative approach of the switchable solvent system, where microcrystalline cellulose is converted in the presence of carbon dioxide (CO_2) and a guanidine superbase, i.e. 1,8-diazabicyclo[5.4.0]undec-7-en (DBU) or 1,5,7-triazabicyclo[4.4.0]dec-5-en (TBD), into a DMSO soluble carbonate species, results in low E-factors (1.92) for cellulose acetate synthesis. This approach is therefore frequently used as a more sustainable alternative to using ILs.[3,27]

Depending on the synthetic strategy and employed substrates, FACEs can contain functional groups such as double bonds.[7,28,29] It is well established that fatty acids can be efficiently modified by applying a broad variety of synthetic reaction protocols,[30] e.g. epoxidation,[31] thiol–ene[32,33] or metathesis.[34,35] Another efficient modification strategy fulfilling several aspects of green chemistry is inverse vulcanization.[36–38] Herein, homolytic cleavage of the highly abundant and practically non-toxic waste material elemental sulfur (70 Mt excess p.a. as a byproduct in petroleum refining) at elevated temperatures (140 to 185 °C) enables a radical reaction with alkene-bearing comonomers towards high sulfur content materials.[37,39]

These materials show broad applicability, for instance in energy storage systems such as Li–S batteries, in oil spill remediation, in mercury capture, or as antimicrobial materials.[37,40–42] Alkene bearing comonomers from renewable feedstocks, such as terpenes or triglycerides, for inverse vulcanization have already been investigated.[40,43–49] The inverse vulcanization of alkene bearing cellulose derivatives is however rarely reported.[29,50,51] In 2019, Smith et al. presented the synthesis of cellulose–sulfur composites (80 wt% ≤ sulfur ≤ 99 wt%) by inverse vulcanization of a cellulose ester (CE) containing pendant alkene functionalities.[50] From a sustainability point of view, the approach however suffers from the use of halogenated substrates, i.e. 3-bromo-3methylpropene (rated as environmental hazard), and the release of corrosive byproducts, i.e. hydrobromic acid (HBr), during the cellulose modification. Subsequently, in 2020 Smith et al. developed a more sustainable three-step procedure for the synthesis of cellulose–sulfur composites (80 wt% ≤ sulfur ≤ 90 wt%), where the C_6-position of native cellulose was first selectively oxidized using sodium hypochlorite, then esterified with a terpenoid, i.e. geraniol, and subsequently inversely vulcanized.[51] By applying the previously described synthetic method, a total atom economy of 90% could be achieved over all three steps. However, particularly the reaction time required for the C_6 oxidation of cellulose, i.e. 14 days, and the following tedious work up remain critical points in terms of energy efficiency and waste production in the approach.

Thus, we herein take advantage of a more sustainable one step synthesis protocol targeting fully renewable FACEs with adjustable DS, which are prominent comonomers for inverse vulcanisation by using a DMSO/TBD/CO_2 switchable solvent system and biobased methyl-10-undecenoate as a trans-esterification agent.[7] High sulfur content (95%) composite materials have been synthesized via inverse vulcanization (E-factor = 0) including FACEs with three different DS (0.38 ≤ DS ≤ 0.62) as comonomers. In-depth structural characterization, i.e. differential scanning calorimetry (DSC), thermogravimetric analysis (TGA), energy dispersive X-ray (EDX) spectroscopy, and scanning electron microscopy (SEM), has been performed especially for the crosslinked sections, supplemented by the investigation of structure–property relationships, i.e. thermal stability (via TGA), hydrophobicity (via WCA) and mercury uptake of the high content sulfur composite materials.

Results and discussion

Using the so-called derivative approach (see Introduction) for cellulose modification in a DMSO/TBD/CO_2 switchable solvent system, cellulose (microcrystalline, dried at 100 °C at 10 mbar overnight) was esterified with biobased methyl-10-undecenoate (Scheme 1A). By applying different amounts of methyl-10-undecenoate (i.e. 2.00, 3.50 and 9.00 equivalents), FACE-1, FACE-2 and FACE-3, respectively, were obtained.
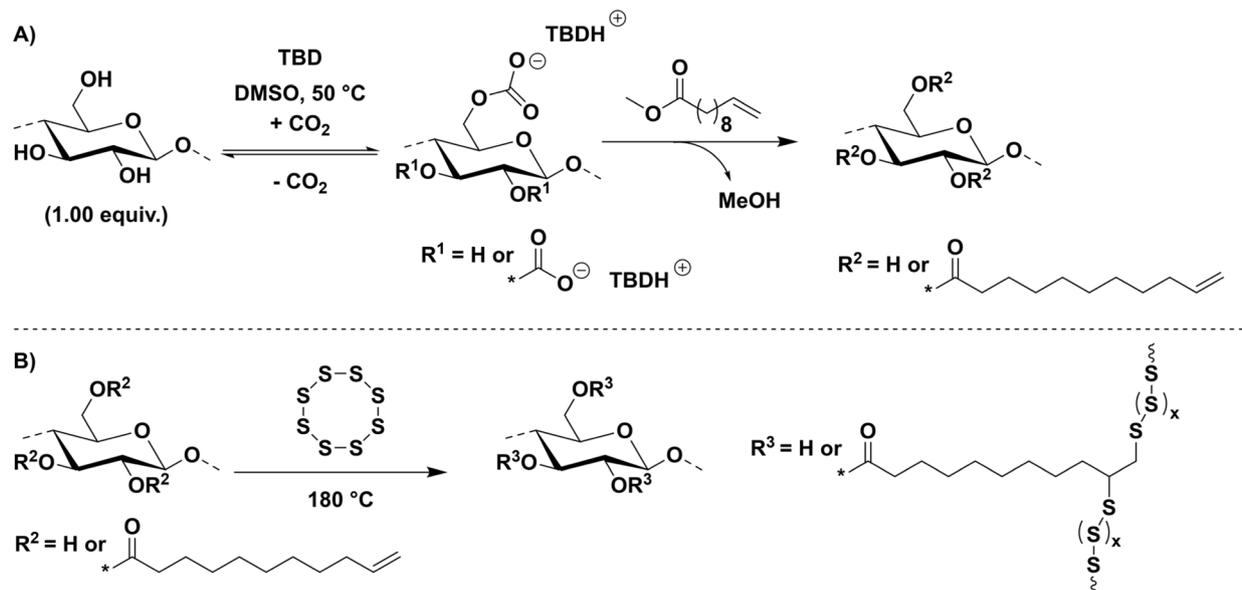
Scheme 1 (A) General concept for cellulose dissolution in a DMSO/TBD/CO$_2$ switchable solvent system with subsequent transesterification using methyl-10-undecenoate to fatty acid cellulose esters (FACE). (B) Synthetic approach for the inverse vulcanization of FACEs towards high sulfur content composite materials.

The structural characterization of these FACES was performed by attenuated total reflection infrared (ATR-IR) spectroscopy supplemented by ^{1}H and ^{31}P nuclear magnetic resonance (NMR) spectroscopy. ATR-IR spectra of all synthesized FACEs (Fig. S1†) revealed characteristic stretching vibration bands at ~1641 cm^{-1} (C=C, Fig.S1†) and ~1730 cm^{-1} (C=O, Fig. S1†), indicating the successful incorporation of ester and alkene functional groups into cellulose. In ^{1}H NMR (Fig. S2–S4†), magnetic resonances appearing from 2.95 to 5.64 ppm, assigned to the unmodified protons of the (AGU), and magnetic resonances at 4.97 ppm and 5.80 ppm, attributed to the introduced double bond protons, additionally confirmed the success of the synthetic approach. The following DS determination of the synthesized FACE materials was conducted according to an established ^{31}P NMR spectroscopy method (Fig. S5–S7†). Thus, the free hydroxyl groups of the respective FACE were converted into phosphite esters by reaction with the phosphitylation agent 2-chloro-4,4,5,5-tetramethyl-1,3,2-dioxaphospholane (2-Cl-TMDP). A subsequent quantitative determination of the corresponding phosphite esters *via* ^{31}P NMR spectroscopy using an internal standard (*endo-N*-hydroxy-5-norbornene-2,3-dicarboximide) allowed the calculation of the average DS as previously reported by Kilpeläinen *et al.* (eqn (S3), (S4) and Fig. S5–S7†).[52] Unsurprisingly, the DS of the synthesized FACEs correlated with the amount of employed transesterification agent, *i.e.* methyl-10-undecenoate. Thus, FACE-1 appeared as the material with the lowest DS, *i.e.* 0.38, followed by FACE-2 (DS = 0.42) and FACE-3 (DS = 0.62), respectively. Conventional inverse vulcanization is usually conducted at elevated temperatures above 160 °C. Therefore, to evaluate if the synthesized FACEs can potentially be employed as comonomers for inverse vulcanization, the thermal properties of the respective materials were investigated *via* TGA (Fig. S8†) and DSC (Fig. S9†). As

shown in Fig. S8 of the ESI,† TGA curves revealed a higher thermal stability for FACEs with lower DS. The higher degradation temperatures, which are defined as the temperature of 5% weight loss ($T_{d,5\%}$), can be explained by the inherently existing strong intra- and intermolecular interactions (predominantly hydrogen bonding) between the hydroxyl groups of the cellulose backbones. An increased amount of incorporated bulky alkyl side chains, *i.e.* a higher DS, affords a partial interruption of the intra- and intermolecular interactions between the cellulose backbones and therefore explains the slightly lower thermal stability of FACE-3 ($T_{d,5\%}$ = 221 °C). DSC measurements of all synthesized FACEs did not show any thermal transition. Size exclusion chromatography (SEC) was performed to determine the molecular weight of the FACEs. Unfortunately, FACE-1 was not soluble in the available SEC eluent, *i.e.* hexafluoro isopropanol (HFIP), and therefore no measurement could be conducted. SEC traces of FACE-2 and FACE-3 (Fig. S10†) revealed high molecular weights (53 kDa ≤ M_n ≤ 64 kDa; 1.85 ≤ Đ ≤ 1.99), a result of the mild reaction conditions during the modification approach using the switchable solvent system,[3] *i.e.* less backbone degradation, which is also beneficial for the material properties. The thermal and structural characterization of the FACEs revealed that they are potential fully renewable comonomers for inverse vulcanization, which was an aim of this study (Scheme 1B).

Therefore, the corresponding FACEs (5 wt%) were mixed with elemental sulfur (95 wt%) and reacted for 24 h at 180 °C. The optical appearance of the final composite materials, *i.e.* FACE-1S, FACE-2S and FACE-3 (Fig. 1) was brown to black. At this point it is worth mentioning that the synthesis of the cellulose-based high sulfur content composite materials was achieved without the employment of any solvent, toxic chemicals, purification steps, and most importantly without the

Fig. 1 Optical appearance of the synthesized high sulfur content composite materials FACE-1S, FACE-2S, and FACE-3S.

production of any waste, and thus an *E*-factor of 0 is the result of this synthesis procedure. First, the thermal properties of the obtained inverse vulcanizates were investigated by conducting DSC measurements (Fig. S11†). Herein, the synthesized composite materials revealed a thermal transition, *i.e.* a significant melting peak, at 120 °C, indicating the presence of unreacted crystalline elemental sulfur.

Accordingly, DSC measurements did not confirm if the expected reaction between the FACE comonomers and elemental sulfur proceeded successfully. For a more detailed understanding of the network structure, unreacted elemental sulfur was thus removed from the synthesized materials to obtain and characterize the formed crosslinked networks. Hence, a washing procedure implementing carbon disulfide (CS_2), which is known to dissolve elemental sulfur at room temperature, was applied to the obtained inverse vulcanizates. Subsequent DSC measurements of the potentially crosslinked residual materials, *i.e.* FACE-1S-washed, FACE-2S-washed, and FACE-3S-washed, did not show any melting peak at 120 °C (Fig. S12†), indicating that no crystalline elemental sulfur remained after the washing procedure. However, potentially covalent incorporation of sulfur could not be confirmed *via* DSC. Interestingly, a two-step degradation behaviour was observed by TGA after sulfur extraction (Fig. 2A). It can be assumed that the first degradation step corresponds to the degradation of covalently incorporated S–S moieties, whereas the second one is attributed to the degradation of the FACE backbone. Correspondingly, with increasing DS of the FACEs, the intensity of the first degradation step (corresponding to the decomposition of S–S bonds) also increased from 5.64 wt% in FACE-1S-washed to 56.2 wt% for FACE-3S-washed. In other words, the amount of covalently incorporated sulfur was related to the DS of the employed FACE comonomer and increased with increasing DS. The previously investigated phenomenon might be explained by the more hydrophobic character of the FACE containing higher DS, which enabled an improved solubility in
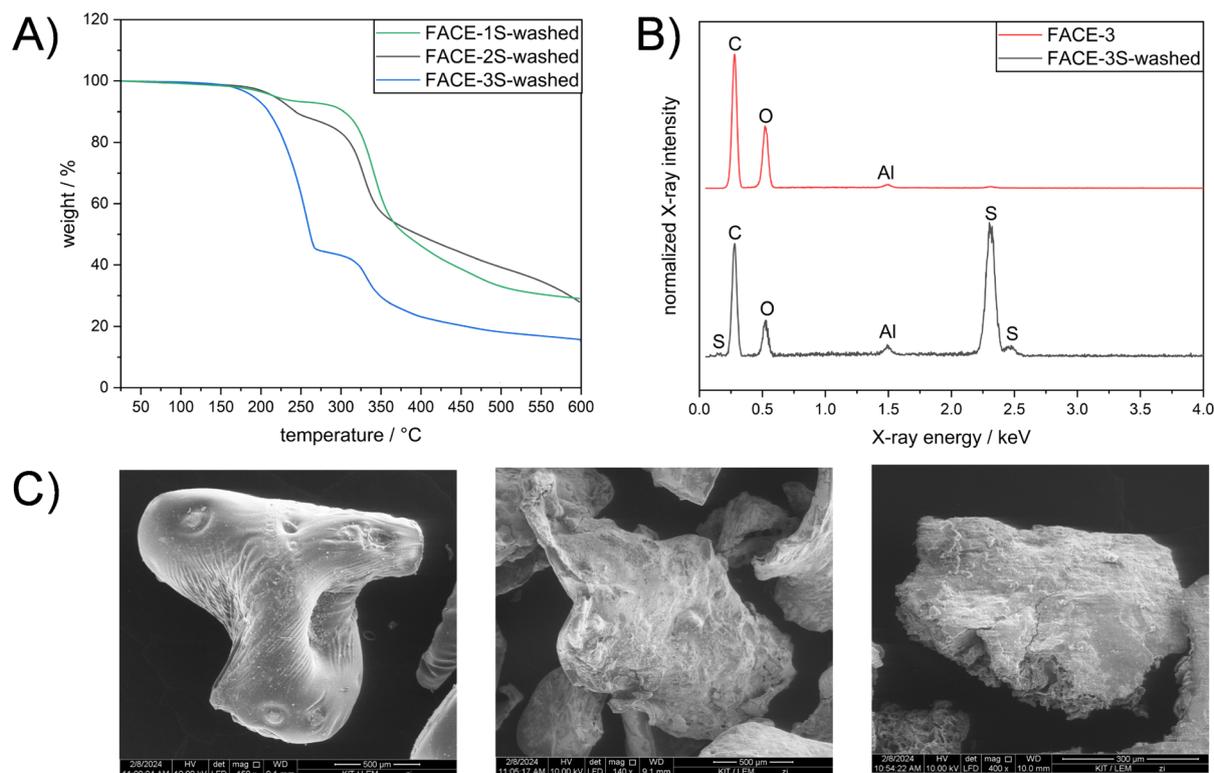

Fig. 2 (A) TGA curves of FACE-1S-washed (green line), FACE-2S-washed (black line), and FACE-3S-washed (blue line) from 25 to 600 °C with a heating rate of 10 K min^{-1} under a nitrogen flow. (B) EDX spectra of FACE-3 (red line) and FACE-3S-washed (black line). (C) SEM pictures of FACE-1S-washed (middle), FACE-2S-washed (right) and FACE-3S-washed (left).
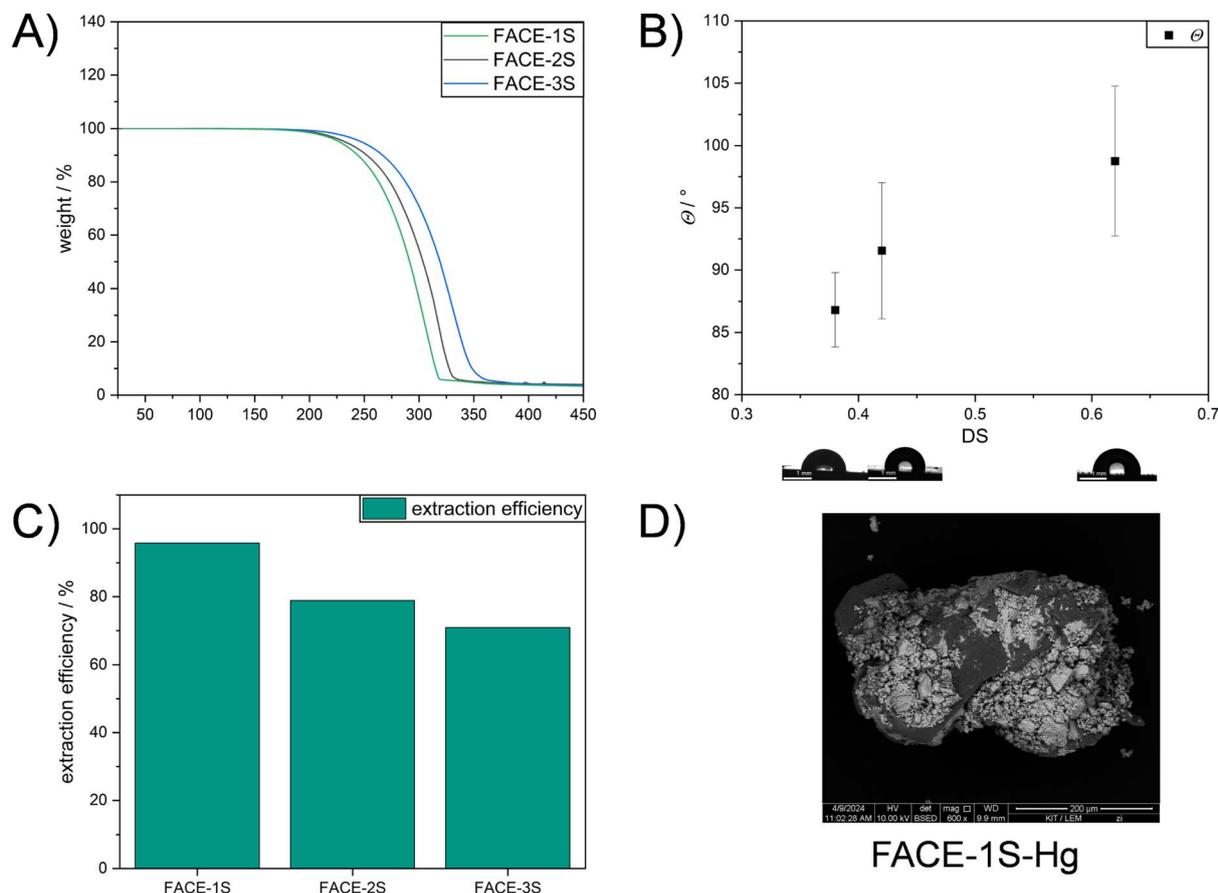
Fig. 3 (A) TGA curves of FACE-1S (green line), FACE-2S (black line), and FACE-3S (blue line). (B) Static WCA measurements of FACE-1S, FACE-2S, and FACE-3S. (C) Mercury removal efficiency of FACE-1S, FACE-2S, and FACE-3S from an aqueous HgCl$_2$ solution (1.00 mg L^{-1}) after 24 h at ambient temperature. (D) Backscattered electron image of FACE-1S after mercury uptake *via* SEM.

molten sulfur and thus a more efficient reaction, *i.e.* covalent implementation of sulfur.

In order to verify the presence of covalently incorporated sulfur in the residue materials, FACE-*X*S-washed ($X = 1, 2$ or 3) were investigated by energy-dispersive X-ray (EDX) spectroscopy. EDX spectra of the FACE comonomers before inverse vulcanization revealed characteristic bands for the elements carbon and oxygen (Fig. 2B, S13 and S14†), which was expected according to their chemical structure (depicted in Scheme 1A). Additional bands for FACE-*X*S-washed particularly appeared between 2.0 and 2.5 keV (Fig. 2B, S13 and S14†), confirming the existence of sulfur in the washed materials. The absence of sulfur crystals in supplemental SEM images of the previously mentioned residue materials combined with smooth surface areas confirmed that the sulfur species, which were detected by EDX, were covalently incorporated (Fig. 2C).

After understanding the formed network structure and confirming that cross-linked composite materials were formed, structure–property relationships were examined. An increased degradation temperature (temperature at which 5% weight loss occurred) was observed by TGA if FACEs with higher DS were incorporated as comonomers (Fig. 3A). More precisely, FACE-1S ($DS_{FACE-1} = 0.38$) revealed the lowest degradation temperature ($T_{d,5\%} = 227$ °C) followed by FACE-2S ($T_{d,5\%} = 233$ °C) and

FACE-3S ($T_{d,5\%} = 247$ °C), respectively. The improved thermal stability of the composite materials including FACEs with higher DS resulted from the increased amount of covalently bonded sulfur (5.67, 12.2 and 56.2 wt% for FACE-1S, FACE-2S, and FACE-3S, respectively) and thus more extensive cross-linking. Interestingly, the composite materials show a one-step degradation behaviour, resulting from the high sulfur content that prevents the observation of the FACE degradation step. The hydrophobic character of FACE-1S, FACE-2S, and FACE-3S was investigated by conducting static WCA measurements (Fig. 3B). In the current literature,[53] it has been frequently described that an increased DS leads to a higher hydrophobicity for CEs. Hence, it was not surprising that the static contact angles increased from 87° for FACE-1S ($DS_{FACE-1} = 0.38$) to 99° for FACE-3S ($DS_{FACE-2} = 0.62$).

Inverse vulcanized materials are known as excellent heavy metal sorbents and can therefore be applied in water purification processes.[45–47,54–56] Thus, to emphasize a potential application for the synthesized high sulfur content composite materials, their potential for mercury uptake from an aqueous HgCl$_2$ solution ($C_i = 1$ mg L^{-1}) was investigated. The chemical structure, *i.e.* the DS of the incorporated FACE comonomers, revealed a significant impact on the extraction efficiency and capacity of the materials (Table 1). As shown in Fig. 3C, FACE-1S

Table 1 Summary of mercury sorption studies of cellulose-based high sulfur content composite materials

Material	Extraction efficiency[a]/%	Distribution coefficient/mL g^{-1}	Extraction capacity/mg g^{-1}
FACE-1S	95	1.13×10^4	0.48
FACE-2S	78	1.87×10^3	0.39
FACE-3S	70	1.22×10^3	0.35

[a] From an aqueous HgCl$_2$ solution ($C_i = 1.00$ mg L^{-1}) after 24 h at ambient temperature.

synthesized from FACE-1 occurred as the most efficient mercury sorbent with an extraction efficiency up to 95%, followed by FACE-2S (78%) and FACE-3S (70%), respectively. The equilibrium mercury concentrations were subsequently employed for the calculation of the distribution coefficient (K_d), which assess the affinity of the synthesized sorbents for Hg^{2+} ions. K_d values can generally be calculated according to eqn (1):

$$K_d = \frac{(C_i - C_f)}{C_f} \times \frac{V}{m} \tag{1}$$

Here, C_i is the initial mercury concentration (mg L^{-1}), C_f is the final mercury concentration (mg L^{-1}), V is the volume of mercury solution (mL), and m is the mass of polymer (g). In line with the investigated extraction efficiencies, FACE-1S possessed the highest calculated K_d of 1.13×10^4 mL g^{-1}, followed by FACES$_{95}$-2 (1.87×10^3 mL g^{-1}) and FACE-3S (1.22×10^3 mL g^{-1}), respectively. Excellent and commercially available mercury sorbents usually exhibit K_d values > 10^5 mL g^{-1}. Thus, particularly FACE-1S ($K_d = 1.13 \times 10^4$ mL g^{-1}) can be categorized as a promising mercury sorbent.

The equilibrium extraction capacities (q_e) of all synthesized composite materials can be calculated according to eqn (2):

$$q_e = (C_i - C_f) \times \frac{V}{m} \tag{2}$$

Unsurprisingly, FACE-1S showed the highest q_e (0.48 mg g^{-1}) compared to FACE-2S (0.39 mg g^{-1}) and FACE-3S (0.35 mg g^{-1}). As a final proof for the adsorption of mercury at the surfaces of the sorbent materials, i.e. FACE-1S, FACE-2S, and FACE-3S, backscattered electron (BSE) images after mercury uptake were recorded via SEM (Fig. 3D, S16A and S16B†, respectively). Fig. 3D exemplarily reveals bright and dark surface areas, where the dark spots correspond to the initial composite material and the bright spots represent areas with adsorbed mercury.

Conclusions

In the current work, microcrystalline cellulose was solubilized in a DMSO/TBD/CO$_2$ switchable solvent system and subsequently transesterified by using the biobased transesterification agent methyl-10-undecenoate by adopting a literature known procedure.[7] Upon the synthesis of renewable FACEs containing

three different DS ($0.38 \leq$ DS ≤ 0.62), in-depth structural characterization, i.e. ^{1}H NMR, ^{31}P NMR, ATR-IR, DSC and TGA, was conducted. The subsequent inverse vulcanization of the synthesized FACEs resulted in high sulfur content composite materials (~95 wt% sulfur). A detailed investigation of the structural composition of the crosslinked sections via DSC, TGA, EDX, XPS and SEM showed an increased amount of covalently implemented sulfur (5.67 wt% $\leq$ wt% sulfur $\leq$ 56.2 wt%), depending on the DS of the employed FACE. Additionally, it was also shown that the structural compositions of the FACEs, i.e. their DS, also influence the material properties of the synthesized high sulfur content composite materials. More precisely, a higher DS of the used FACEs afforded a higher thermal stability (227 °C $\leq T_{d,5\%} \leq$ 247 °C), an elevated surface hydrophobicity (87° $\leq \theta \leq$ 99°) and a lower mercury extraction efficiency (70% $\leq$ Hg$_{removal}^{2+} \leq$ 95%).

Experimental part

Materials

Microcrystalline cellulose (MCC, Sigma-Aldrich) was dried under reduced pressure at 100 °C for 24 hours prior to use. Dimethyl sulfoxide (DMSO, dried and stored over molecular sieves, Acros Organics, >99.7%), 1,5,7-triazabicyclo[4.4.0]dec-5-ene (TCI, ≥98%), methanol (VWR, ≥99.8%), methyl-10-undecenoate (Sigma-Aldrich, 96%), endo-N-hydroxy-5-norbornene-2,3-dicarboximide (Alfa Aesar, 97%), DMSO-d_6 (Eurisotop, 99.8%), and CDCl$_3$ (Eurisotop, 99.8%) were used without further purification. 2-Chloro-4,4,5,5-tetramethyl-1,3,2-dioxaphospholane (2-Cl-TMDP) was synthesized according to a literature known procedure.

General procedure for the synthesis of FACEs

Fatty acid cellulose esters (FACEs) were synthesized according to a literature known procedure.[7]

Accordingly, microcrystalline cellulose (MCC, 0.50 g, 1.50 mmol) was suspended in 10 mL anhydrous DMSO in a two neck round bottom flask. Subsequently, TBD (1.28 g, 9.25 mmol) was added, and the reaction mixture was stirred after applying a continuous CO$_2$ flow for 20 minutes at 50 °C. The homogeneous solution was then heated to 95 °C and methyl-10-undecenoate (2.00 equiv., 3.50 equiv. and 9.00 equiv. per AGU for FACE-1, FACE-2, and FACE-3, respectively.) was added in a dropwise manner. The dark brown mixture was stirred for 6 h under air flow, diluted with 10 mL of anhydrous DMSO and precipitated under vigorous stirring in 200 mL of water. The residue was filtered, stirred in methanol, again filtered and subsequently dried under reduced pressure at 80 °C. The corresponding yields were determined depending on the DS$_{31P}$ according to eqn (S1) and (S2).†

FACE-1 (DS = 0.38): yield: 43% ATR-IR: ν (cm^{-1}) = 3644–3035 ν(O–H), 3009–2789 ν(C–H), 1728 ν(C=O), 1639 ν(C=C), 1016 ν(C–O)$_{AGU}$. ^{1}H NMR (400 MHz, DMSO-d_6) δ (ppm) = 5.79 (br, H$_f$, 1H), 5.52–2.96 (m, AGU, 7H), 4.96 (br, H$_e$, 2H), 2.32 (br, H$_d$, 2H), 2.01 (br, H$_c$, 2H), 1.51 (br, H$_b$, 2H), 1.38–1.17 (br, H$_a$, 10H).

FACE-2 (DS = 0.42): yield 51.6% ATR-IR: ν (cm^{-1}) = 3653–3029 ν(O–H), 3003–2799 ν(C–H), 1728 ν(C=O), 1639 ν(C=C), 1016 ν(C–O)$_{AGU}$. ^{1}H NMR (400 MHz, DMSO-d_6) δ (ppm) = 5.79 (br, H$_f$, 1H), 5.56–2.96 (m, AGU, 7H), 4.96 (br, H$_e$, 2H), 2.32 (br, H$_d$, 2H), 2.01 (br, H$_c$, 2H), 1.51 (br, H$_b$, 2H), 1.40–1.15 (br, H$_a$, 10H).

FACE-3 (DS = 0.62): yield 58.6% ATR-IR: ν (cm^{-1}) = 3651–3105 ν(O–H), 3013–2793 ν(C–H), 1734 ν(C=O), 1639 ν(C=C), 1016 ν(C–O)$_{AGU}$. ^{1}H NMR (400 MHz, DMSO-d_6) δ (ppm) = 5.78 (br, H$_f$, 1H), 5.61–2.82 (m, AGU, 7H), 4.94 (br, H$_e$, 2H), 2.32 (br, H$_d$, 2H), 2.00 (br, H$_c$, 2H), 1.51 (br, H$_b$, 2H), 1.40–1.15 (br, H$_a$, 10H).

General procedure for DS determination via ^{31}P NMR spectroscopy

An exact amount of the corresponding FACE (20 mg) was dissolved in 1.00 mL of pyridine. Subsequently, 1.00 mL of CDCl$_3$ and 200 μL of 2-chloro-4,4,5,5-tetramethyl-1,3,2-dioxaphospholane (2-Cl-TMDP, 1.26 mmol) were added and the reaction mixture was stirred until a visibly homogeneous solution was obtained. After adding the internal standard endo-N-hydroxy-5-norbornene-2,3-dicarboximide (125 μL, 105.59 mM in pyridine/CDCl$_3$ = 3 : 2, 0.0132 mmol) the solution was again stirred for at least 10 minutes before 0.60 mL was transferred into an NMR tube and ^{31}P NMR was conducted. The DS values were calculated according to Kilpeläinen et al.[52] by applying eqn. (S3) and (S4).†

General procedure for the synthesis of FACES$_{95}$

A crimp vial was charged with elemental sulfur (2.85 g, 95.0 wt%) and the corresponding FACE (150 mg, 5.00 wt%). Subsequently, the reaction mixture was heated to 180 °C and stirred for 24 h until the black reaction medium appeared homogeneous. After cooling to room temperature, the targeted composite materials were obtained.

FACE-1S: yield: 100%
FACE-2S: yield: 100%
FACE-3S: yield: 100%

General procedure for mercury sorption studies

200 mg of the respective high sulfur content composite material was crushed into a powder and subsequently added to 100 mL of an aqueous HgCl$_2$ solution (C_i = 1.00 mg L^{-1}). After stirring the solution for 24 h at ambient temperature, the inverse vulcanized material was filtered off and the mercury concentration in the solution was determined via Cold Vapor Atomic Absorption spectroscopy.

Instrumentation

Infrared spectroscopy (IR). Infrared spectra were recorded using a Bruker Alpha-p instrument with ATR technology in a range of ν = 500–4000 cm^{-1} with 24 scans per measurement.

Nuclear magnetic resonance (NMR) spectroscopy. ^{1}H NMR spectra were recorded using a Bruker Ascend 400 MHz with 16 scans and a delay time d1 of 5 seconds at 298 K. The chemical shift was reported in ppm and referenced to the solvent signal of partly deuterated DMSO-d_6 at 2.50 ppm. ^{31}P NMR spectra

were recorded using a Bruker Ascend instrument at 162 MHz with 1024 scans and a delay time d1 of 5 seconds at 298 K.

Size exclusion chromatography (SEC). SEC measurements were performed in HFIP containing 0.1 wt% potassium trifluoroacetate (KTFA) using a Tosoh EcoSEC HLC8320 SEC system. The solvent flow was 0.40 mL min^{-1} at 30 °C, and the concentration of the samples was 1 mg mL^{-1}. The analysis was performed using a three-column system: PSS PFG Micro precolumn (3.0 × 0.46 cm, 10 000 Å), PSS PFG Micro (25.0 × 0.46 cm, 1000 Å), and PSS PFG Micro (25.0 × 0.46 cm, 100 Å). The system was calibrated with linear poly(methyl methacrylate) standards (Polymer Standard Service, M_p: 102–981 kDa).

Differential scanning calorimetry (DSC). DSC measurements were performed on a Mettler Toledo DSC821e instrument using 100 μL aluminium crucibles under a nitrogen atmosphere. The samples were measured in two heating cycles: 25–150 °C, 150 to −40 °C and −40–150 °C at a heating/cooling rate of 10 K min^{-1}. The second heating cycle is shown in the DSC curves.

Thermogravimetric analysis (TGA). TGA measurements were carried out on a TA Instruments TGA 5500 under a nitrogen atmosphere using platinum TGA sample pans and with a heating rate of 10 K min^{-1} over temperature ranges from 25 °C to 500 °C, 25 °C to 600 °C and 25 °C to 450 °C for FACEs, FACE-XS-washed and FACE-XS, respectively.

Energy dispersive X-ray (EDX) spectroscopy. For EDX spectroscopy, a QUANTAX (Esprit 1.9) from Bruker was used.

Scanning electron microscopy (SEM). For SEM analysis, the samples were sputtered with a thin layer of carbon. All analysed materials were investigated with a QUANTA FEG 650 scanning electron microscope from FEI with an accelerating voltage of 5–10 kV.

Water contact angle (WCA) measurements. Contact angle measurements were performed with a DSA 25 contact angle goniometer (Krüss) using the sessile drop technique. A water droplet with a size of 5 μL was slowly added on the materials using a micrometer syringe and contact angles of the materials against the water droplet were measured. The average value of five measurements was calculated for each sample with a standard deviation between 3° and 6°.

Atomic absorption spectrometry (AAS). Cold-vapor AAS measurements were performed using a QuickTrace M-7600 from Teledyne Leeman Labs. A bromination reagent was added prior to measurements.

Data availability

The data supporting this article have been included within the article and as part of the ESI.†

Author contributions

Timo Sehn: conceptualization, formal analysis, investigation, writing – original draft; Julian Fanelli: investigation (synthesis), writing – review & editing; Lisa Wahl: investigation (synthesis); Michael A. R. Meier: project administration, supervision, writing – review & editing.

Conflicts of interest

There are no conflicts to declare.

Acknowledgements

References

1 P. Anastas and J. Warner, *Green Chemistry: Theory and Practice*, Oxford University Press, New York, 1998.

2 P. Anastas and N. Eghbali, *Chem. Soc. Rev.*, 2010, **39**, 301–312.

3 J. Wolfs and M. A. R. Meier, *Green Chem.*, 2021, **23**, 4410–4420.

4 D. Klemm, B. Heublein, H.-P. Fink and A. Bohn, *Angew. Chem., Int. Ed.*, 2005, **44**, 3358–3393.

5 T. Sehn and M. A. R. Meier, *Biomacromolecules*, 2023, **24**, 5255–5264.

6 S. Mi, Z. Yao, F. Liu, Y. Li, J. Wang, H. Na and J. Zhu, *Green Chem.*, 2022, **24**, 8677–8684.

7 E. Esen, P. Hädinger and M. A. R. Meier, *Biomacromolecules*, 2021, **22**, 586–593.

8 Z. Chen, J. Zhang, P. Xiao, W. Tian and J. Zhang, *ACS Sustainable Chem. Eng.*, 2018, **6**, 4931–4939.

9 S. B. W. Kusuma, D. Hirose, A. Yoshizawa, L. Szabó, D. Ina, N. Wada and K. Takahashi, *ACS Sustainable Chem. Eng.*, 2021, **9**, 8450–8457.

10 A. Schenzel, A. Hufendiek, C. Barner-Kowollik and M. A. R. Meier, *Green Chem.*, 2014, **16**, 3266–3271.

11 H. Steinmeier, *Macromol. Symp.*, 2004, **208**, 49–60.

12 C. L. McCormick, P. A. Callais and B. H. Hutchinson Jr, *Macromolecules*, 1985, **18**, 2394–2401.

13 O. A. El Seoud, G. A. Marson, G. T. Ciacco and E. Frollini, *Macromol. Chem. Phys.*, 2000, **201**, 882–889.

14 R. P. Swatloski, S. K. Spear, J. D. Holbrey and R. D. Rogers, *J. Am. Chem. Soc.*, 2002, **124**, 4974–4975.

15 P. Willberg-Keyriläinen and J. Ropponen, *Heliyon*, 2019, **5**, e02898.

16 X. Cao, S. Sun, X. Peng, L. Zhong, R. Sun and D. Jiang, *J. Agric. Food Chem.*, 2013, **61**, 2489–2495.

17 R. A. Sheldon, *Green Chem.*, 2007, **9**, 1273–1283.

18 T. Kulomaa, J. Matikainen, P. Karhunen, M. Heikkilä, J. Fiskari and I. Kilpeläinen, *RSC Adv.*, 2015, **5**, 80702–80708.

19 L. Duchatel-Crépy, N. Joly, P. Martin, A. Marin, J.-F. Tahon, J.-M. Lefebvre and V. Gaucher, *Carbohydr. Polym.*, 2020, **234**, 115912.

20 M. A. Hussain, T. Liebert and T. Heinze, *Macromol. Rapid Commun.*, 2004, **25**, 916–920.

21 M. C. Nagel and T. Heinze, *Lenzinger Ber.*, 2012, **90**, 85–92.

22 H. Nawaz, R. Casarano and O. A. El Seoud, *Cellulose*, 2012, **19**, 199–207.

23 H. A. Staab, *Angew Chem. Int. Ed. Engl.*, 1962, **1**, 351–367.

24 M. Jebrane, N. Terziev and I. Heinmaa, *Biomacromolecules*, 2017, **18**, 498–504.

25 K. D. Mekonnen and Z. B. Sendekie, *ACS Omega*, 2021, **6**, 24082–24091.

26 M. Gericke, P. Fardim and T. Heinze, *Molecules*, 2012, **17**, 7458–7502.

27 C. Libretti and M. A. R. Meier, *Macromolecules*, 2023, **56**, 7532–7542.

28 K. N. Onwukamike, S. Grelier, E. Grau, H. Cramail and M. A. R. Meier, *ACS Sustainable Chem. Eng.*, 2018, **6**, 8826–8835.

29 H. Kato, F. Nakatsubo, K. Abe and H. Yano, *RSC Adv.*, 2015, **5**, 29814–29819.

30 U. Biermann, U. T. Bornscheuer, I. Feussner, M. A. R. Meier and J. O. Metzger, *Angew. Chem., Int. Ed.*, 2021, **60**, 20144–20165.

31 J. Chen, M. de Liedekerke Beaufort, L. Gyurik, J. Dorresteijn, M. Otte and R. J. M. Klein Gebbink, *Green Chem.*, 2019, **21**, 2436–2447.

32 Y. H. Zhao, S. Hupin, L. Lecamp, D. Vuluga, C. Afonso, F. Burel and C. Loutelier-Bourhis, *RSC Adv.*, 2017, **7**, 3343–3352.

33 M. Ge, J.-T. Miao, K. Zhang, Y. Wu, L. Zheng and L. Wu, *Polym. Chem.*, 2021, **12**, 564–571.

34 D. Le, C. Samart, K. Tsutsumi, K. Nomura and S. Kongparakul, *ACS Omega*, 2018, **3**, 11041–11049.

35 J. Hobich, B. Huber, P. Theato and H. Mutlu, *Macromol. Rapid Commun.*, 2021, **42**, 2100118.

36 F. G. Müller, L. S. Lisboa and J. M. Chalker, *Adv. Sustainable Syst.*, 2023, **7**, 2300010.

37 W. J. Chung, J. J. Griebel, E. T. Kim, H. Yoon, A. G. Simmonds, H. J. Ji, P. T. Dirlam, R. S. Glass, J. J. Wie, N. A. Nguyen, B. W. Guralnick, J. Park, Á. Somogyi, P. Theato, M. E. Mackay, Y.-E. Sung, K. Char and J. Pyun, *Nat. Chem.*, 2013, **5**, 518–524.

38 M. J. H. Worthington, R. L. Kucera and J. M. Chalker, *Green Chem.*, 2017, **19**, 2748–2761.

39 T. Lee, P. T. Dirlam, J. T. Njardarson, R. S. Glass and J. Pyun, *J. Am. Chem. Soc.*, 2022, **144**, 5–22.

40 A. Hoefling, Y. J. Lee and P. Theato, *Macromol. Chem. Phys.*, 2017, **218**, 1600303.

41 M. K. Lauer, A. G. Tennyson and R. C. Smith, *Mater. Adv.*, 2021, **2**, 2391–2397.

42 A. D. Tikoalu, N. A. Lundquist and J. M. Chalker, *Adv. Sustainable Syst.*, 2020, **4**, 1900111.

43 A. D. Smith, C. D. McMillen, R. C. Smith and A. G. Tennyson, *J. Polym. Sci.*, 2020, **58**, 438–445.

44 J. Jia, J. Liu, Z.-Q. Wang, T. Liu, P. Yan, X.-Q. Gong, C. Zhao, L. Chen, C. Miao, W. Zhao, S. Cai, X.-C. Wang, A. I. Cooper, X. Wu, T. Hasell and Z.-J. Quan, *Nat. Chem.*, 2022, **14**, 1249–1257.

45 M. P. Crockett, A. M. Evans, M. J. H. Worthington, I. S. Albuquerque, A. D. Slattery, C. T. Gibson,

J. A. Campbell, D. A. Lewis, G. J. L. Bernardes and J. M. Chalker, *Angew. Chem., Int. Ed.*, 2016, **55**, 1714–1718.

46 D. J. Parker, H. A. Jones, S. Petcher, L. Cervini, J. M. Griffin, R. Akhtar and T. Hasell, *J. Mater. Chem. A*, 2017, **5**, 11682–11692.

47 M. J. H. Worthington, R. L. Kucera, I. S. Albuquerque, C. T. Gibson, A. Sibley, A. D. Slattery, J. A. Campbell, S. F. K. Alboaiji, K. A. Muller, J. Young, N. Adamson, J. R. Gascooke, D. Jampaiah, Y. M. Sabri, S. K. Bhargava, S. J. Ippolito, D. A. Lewis, J. S. Quinton, A. V. Ellis, A. Johs, G. J. L. Bernardes and J. M. Chalker, *Chem.–Eur. J.*, 2017, **23**, 16219–16230.

48 M. J. H. Worthington, C. J. Shearer, L. J. Esdaile, J. A. Campbell, C. T. Gibson, S. K. Legg, Y. Yin, N. A. Lundquist, J. R. Gascooke, I. S. Albuquerque, J. G. Shapter, G. G. Andersson, D. A. Lewis, G. J. L. Bernardes and J. M. Chalker, *Adv. Sustainable Syst.*, 2018, **2**, 1800024.

49 C. V. Lopez, M. S. Karunarathna, M. K. Lauer, C. P. Maladeniya, T. Thiounn, E. D. Ackley and R. C. Smith, *J. Polym. Sci.*, 2020, **58**, 2259–2266.

50 M. K. Lauer, T. A. Estrada-Mendoza, C. D. McMillen, G. Chumanov, A. G. Tennyson and R. C. Smith, *Adv. Sustainable Syst.*, 2019, **3**, 1900062.

51 M. K. Lauer, A. G. Tennyson and R. C. Smith, *ACS Appl. Polym. Mater.*, 2020, **2**, 3761–3765.

52 A. W. T. King, J. Jalomäki, M. Granström, D. S. Argyropoulos, S. Heikkinen and I. Kilpeläinen, *Anal. Methods*, 2010, **2**, 1499–1505.

53 M. Ioelovich, *Polymers*, 2021, **13**, 1241.

54 X. Wu, J. A. Smith, S. Petcher, B. Zhang, D. J. Parker, J. M. Griffin and T. Hasell, *Nat. Commun.*, 2019, **10**, 647.

55 M. J. H. Worthington, M. Mann, I. Y. Muhti, A. D. Tikoalu, C. T. Gibson, Z. Jia, A. D. Miller and J. M. Chalker, *Phys. Chem. Chem. Phys.*, 2022, **24**, 12363–12373.

56 J. M. Chalker, M. Mann, M. J. H. Worthington and L. J. Esdaile, *Org. Mater.*, 2021, **03**, 362–373.